24th INTERNATIONAL CONGRESS ON SOUND AND VIBRATION
23–27 July 2017, London

ON NUMERICAL ANALYSIS AND EXPERIMENT VERIFICATION OF CHARACTERISTIC FREQUENCY OF ANGULAR CONTACT BALL-BEARING IN HIGH SPEED SPINDLE SYSTEM

Tian-Yau Wu and Chun-Che Sun

Department of Mechanical Engineering, National Chung Hsing University, Taichung City, Taiwan
email: tianyauwu@dragon.nchu.edu.tw

Yi-Cheng Chen

Department of Mechanical Engineering, National Central University, Taoyuan City, Taiwan

The purpose of this research is to analyze the characteristics frequencies of angular-contact ball-bearing used in high-speed spindle system under the running conditions of different preloads and rotating speeds. A number of dynamic states are investigated, consisting of the equilibrium among the centrifugal force, gyroscopic moment and ball-race contact forces, and the geometric relationship of contact deformation. By solving the equations of the dynamic states, the contact angles between the rolling ball and the inner/outer race are estimated under the running conditions of different preloads and rotating speeds. Using the estimated contact angles, the characteristic frequencies of bearing can be determined. The numerical results of the characteristic frequencies are compared with the analysis results of vibration measurements in the experiment. The spectral features of different bearing defects are extracted by means of the empirical mode decomposition method as well as the fast-Fourier transform (FFT) algorithm.

Keywords: high-speed spindle, preload, bearing defect diagnosis, angular-contact ball-bearing

1. Introduction

Bearing is one of the important components in the rotating machinery for its capability of sustainment as well as transmission. The running conditions of bearings are crucial to the performance of the spindle systems and thus the researchers and engineers have dedicated more and more research energy to the technology development of the bearing diagnosis and prognosis. Among the several techniques, the analysis of vibration signal is the major means for the machine fault diagnostics as well as the condition monitoring since the vibration signals contain plentiful system dynamics related information.

Hertz [1] investigated the contact forces between the rolling balls and races (outer and inner races) of bearing through the classic elasticity analysis. It was the fundamental theory for the ball bearing to derive the relationship between the stress and the deformation of the elliptic surface. The Stribeck's equation was formulated to express the maximum normal force of ball bearing as a function of the radial load, rolling ball number and the contact angle [2].

The centrifugal force and gyroscopic moment that are produced from the bearing dynamic load are generally negligible in case of low rotating speed. Under the conditions of high rotating speeds, however, the increased centrifugal forces of rolling balls enlarge the load difference between the

ball contact surfaces on the inner and on the outer races of ball bearing. The effect of gyroscopic moment increases the friction forces of the ball contact surface concurrently. Therefore, all the contact angle between the rolling ball and the inner race, the contact angle between the rolling ball and the outer race and the ball contact surface deformation change correspondingly under the conditions of high rotating speed. Jones [3] constructed the mathematical expressions for the dynamics of bearing components. Thereafter, the analytical model of ball bearing was derived in terms of the radial load, the axial load and the centrifugal force of the rolling ball. Based on the Hertz contact theory, Harris [4] formulated the deformation of bearing components through considering the ball centrifugal force, the friction force, the radial and the axial loads. The relationship between the bearing loads and its deformation was also studies, in which both the preload and the backlash in the axial direction were involved in the analysis [5].

A proper axial preload is generally applied to the angular-contact ball-bearing for the purpose of decreasing the effects of the bearing component clearance and increasing the stiffness of the spindle system. The derivations of the contact angles and the component loads of the angular-contact ball-bearing for different axial preloads have been summarized by Harris [4]. Furthermore, Antoine et al. [6] investigated the mathematical expressions for the dynamics analysis of the angular-contact ball- bearing. In their studies, the contact angles between the rolling ball and the bearing raceways (inner and outer races) were described through the geometric relationship analysis of bearing components and the dynamics formulations that are parametrized by the preload and shaft rotating speed.

It is well-known that the characteristic frequencies of defective bearing are governed by the geometric properties of bearing as well as the shaft rotating speed. It is also noted that the contact angles of the angular-contact ball-bearing change with respect to the different preloads and the shaft rotating speed in the high-speed spindle system. Namely, the characteristic frequencies of defective bearings in high-speed spindle systems are the complicated nonlinear functions of rotating speed and preload. Therefore, the objective of this research is to utilize the genetic algorithm (GA) optimization method for solving the contact angles of the angular-contact ball-bearing under different rotating speed and axial preload in high-speed spindle system. The theoretical characteristic frequencies of defective bearing are then derived accordingly. The vibration signals that measured from the high-speed bearing test rig were then analysed to verify the characteristic frequencies of the defective angular-contact ball-bearing experimentally. The experimental data demonstrated that the vibration energy concentration can be observed at the corresponding characteristic frequencies whose values are close to the numerical results within a tolerance of 10%.

2. Theoretical model of angular-contact ball-bearing

The dynamics analysis for the angular-contact ball-bearing is derived based on the geometric relationship of bearing components, the contact deformation resulted from the point load, the centrifugal force effect and the associated force/moment equilibrium in the bearing set.

While the shaft rotating speed increases, the centrifugal force and the gyroscopic moment become the major loads on the angular-contact ball-bearing. Therefore, the loads on the inner and outer races acted by the rolling balls are dependent upon the rotating speed, and so is the corresponding deformation. According to the formula in [4], the centrifugal force F_c and the gyroscopic moment M_g can be expressed as

$$\begin{aligned} F_c &= \frac{d_m}{2} m_b \Omega_c \\ M_g &= J_b \Omega_c \Omega_b \sin\beta \ , \\ \tan\beta &= \frac{\sin\alpha_o}{\cos\alpha_o + \frac{d_m}{d_b}} \end{aligned} \tag{1}$$

where $d_{\bullet}$ represents the diameter, $m_{\bullet}$ represents the mass, $\Omega_{\bullet}$ represents the rotating speed, $J_{\bullet}$ represents the moment of inertia, $\alpha_{\bullet}$ represents the contact angle and the subscripts *m*, *b*, *c*, *o* indicate the bearing pitch, ball, cage, and outer race, respectively.

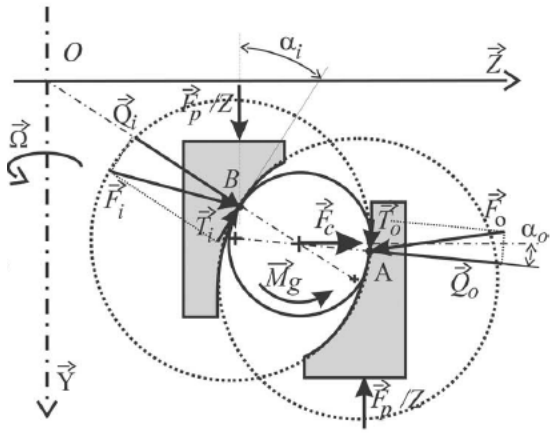

Figure 1 Dynamic state of angular-contact ball-bearing [6]

As shown in Figure 1, Q_i and Q_o are the forces that are acted by the ball on the point A of outer race and on the point B of inner race. Let δ represent the deformation, and hence the relationship between Q and δ can be formulated as [4]

$$Q = K\delta^{1.5}, \tag{2}$$

where K represents the effective elasticity coefficient. The calculation of the effective elasticity coefficients for the inner and outer races can be found in the studies of Houpert [7]. On the other hand, the state of force/moment equilibrium can be summarized as [6]

$$\begin{aligned} Q_o &= \frac{F_p}{Z\sin\alpha_o} + 2\frac{M_g\cos\alpha_o}{d_b\sin\alpha_o} \\ Q_i &= \frac{F_p}{Z\sin\alpha_i} \end{aligned} \tag{3}$$

where F_p is the axial preload and Z is the number of rolling ball. The rotating speed of cage Ω_c can described in terms of the shaft rotating speed Ω and the geometric properties by assuming that the velocity magnitude on A and B is equivalent, that is [6]

$$\Omega_c = \Omega\frac{(d_m - d_b\cos\alpha_i)\cos(\alpha_o - \beta)}{d_m[\cos(\alpha_o - \beta) + \cos(\alpha_i - \beta)] + d_b\sin(\alpha_i - \alpha_o)\sin\beta}. \tag{4}$$

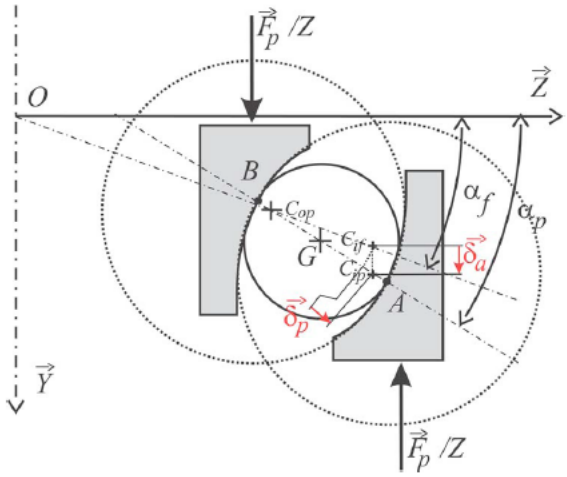

Figure 2 Geometric state of angular-contact ball-bearing [5]

As shown in Figure 2, the preload F_p produces axial force and changes the geometric state of the bearing. The mathematical expression regarding to the geometric state of bearing can be formulated as [5]

$$\begin{aligned}(a_o+\delta_o)\cos\alpha_o+(a_i+\delta_i)\cos\alpha_i&=(a_o+a_i)\cos\alpha_f\\(a_o+\delta_o)\sin\alpha_o+(a_i+\delta_i)\sin\alpha_i&=(a_o+a_i)\sin\alpha_f+\delta_a\end{aligned}\tag{5}$$

where α_f is the initial contact angle, $\delta_{\bullet}$ represents the ball-race deformation, $a_{\bullet}$ represents the distance between the groove curvature and the ball centers, and the subscript i and o represent the inner and outer races, respectively. According to the derivation in [5], δ_a changes with respect to the distance of C_{ip} and C_{op}. It was also indicated that δ_a=0 as applying a fixed preload and high rotating speed.

As the formulae of the bearing states that include the effect of centrifugal force and gyroscopic moment, the load-deformation relationship, the load equilibrium state and the geometric relationship are constructed, the contact angles between the rolling ball and the bearing raceways can be obtained through solving for the independent equations. Since the equations of the different bearing states are nonlinear, the genetic algorithm (GA) optimization approach was utilized in this research to find the numerical solutions of the contact angles under the different axial preload and shaft rotating speed.

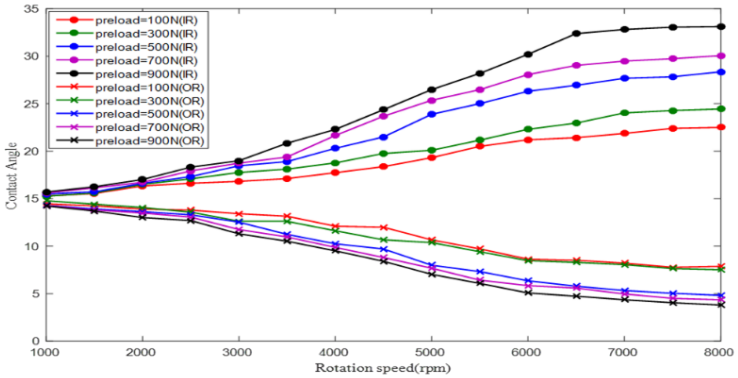

Figure 3 Contact angles of inner (•) and outer (*) races

By setting the different axial preloads and shaft rotating speeds, the numerical solutions to the contact angles α_i and α_o of the bearing TP7014 are obtained as shown in Figure 3. As shown in

Figure 3, the contact angle between the rolling ball and inner race becomes large while increasing the shaft rotating speed under a fixed axial preload. In case of applying a fixed rotating speed, the contact angle between the rolling ball and the inner race increases as the axial preload increases. Contrastively, the contact angle between the rolling ball and the outer race decreases as the increased axial preload and shaft rotating speed.

3. Experiment verification

As shown in Figure 4, a bearing test rig was performed to simulate the different defective running conditions of the TP7014 bearing. The bearing defects were produced artificially on the inner race, outer race and the ball, respectively. The defective bearing was then replaced accordingly for the tests of different running conditions. The vibration amplitude increases while the bearing component impacts the point of bearing defect. Therefore, the vibration energy concentration can be observed at the certain frequency bands that are the major characteristic frequencies utilized for the defective feature extraction as well as the bearing defect diagnostics.

Figure 4 High speed Angular-contact ball-bearing test rig;
1: motor drive; 2: shaft speed sensor; 3: motor; 4: NI9234 DAQ card; 5: NI9219 DAQ card;
6: TP7014 bearing test rig; 7: load cell; 8: LabVIEW interface; 9: accelerometer

According to the mechanism of bearing, the characteristic frequencies related to the bearing defects include the shaft rotation frequency f_r, the cage rotation frequency f_c, the frequency of roller passing through one point of outer race f_{bpo}, the frequency of roller passing through one point of inner race f_{bpi}, the roller spin frequency f_{bs} and the frequency of one point on the roller passing through raceways and cage f_{rp}. The characteristic frequencies can be formulated as

$$f_r = \frac{N}{60}, \tag{6}$$

$$f_c = \frac{\Omega_c}{60}, \tag{7}$$

$$f_{bpo} = Z f_c, \tag{8}$$

$$f_{bpi} = Z\left|f_c - f_r\right|, \tag{9}$$

$$f_{bs} = \left| (f_r - f_c) \frac{\frac{d_m}{2} - \frac{d_b}{2}\cos\alpha_i}{\frac{d_b}{2}\cos(\alpha_i - \beta)} \right|, \tag{10}$$

$$f_{rp} = 3 f_{bs}, \tag{11}$$

where N represents the shaft rotating speed (unit: rpm), Z is the number of roller, r_b represents the radius of roller, r_i represents the radius of inner race and r_o represents the radius of outer race.

The angular-contact ball-bearing with different defects were installed in the high-speed bearing test rig under different combinations of axial preloads and shaft rotating speeds. The accelerometer was utilized to measure the vibrating acceleration and then the vibration signals were captured through the data acquisition device. The axial preload was measured by the load cell. In the experiment, the shaft rotating speed was set to be 1000-6000 rpm with an increment of 500 rpm. According to the specification of TP7014 bearing, the axial preload value is selected as 100-900 N with an increment of 200 N.

The vibration measurements were first decomposed into a number of intrinsic mode functions (IMFs) by the empirical mode decomposition (EMD) method [8]. Through the EMD process, the instantaneous frequency range of each IMF can be determined, and thus the vibration signal components within a certain frequency band can be synthesized by adding the corresponding IMFs. In this research, the vibration signal components whose frequency bands are within the range of the characteristic frequencies were extracted to compose the information-contained signal, so that the signal components which belong to noise or uncorrelated components can be vanished.

The fast Fourier transform (FFT) method was employed for the spectrum analysis of the composed signals. Based on the theoretical model of angular-contact ball-bearing, the contact angles between the rolling ball and the inner/outer races change with the shaft rotating speed as well as the axial preload. Therefore, the characteristic frequencies were determined numerically according to the rotating speed, contact angles and the bearing geometric properties. The spectrum analysis results of the vibration measurements are verified to compare the numerical values of theoretical characteristic frequencies. Figure 5-8 show the spectrum examples of the experimental cases that include the different combinations of shaft rotating speed and axial preload. In the figures, the vertical dash lines from left side to right side represent the numerically determined frequency values of f_c, f_r, f_{bs}, f_{bpo}, f_{bpi} and f_{rp}.

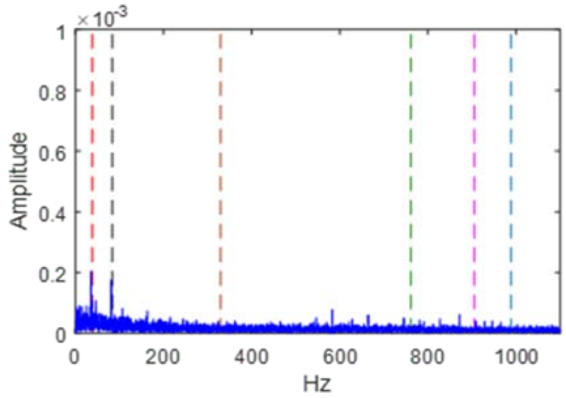

Figure 5 Spectrum of normal bearing; speed=5000 rpm; preload=500 N

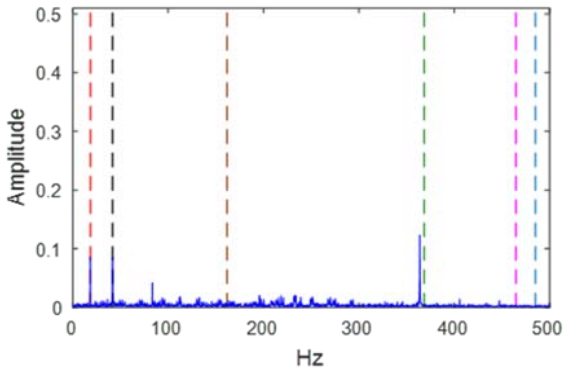

Figure 6 Spectrum of bearing with outer race defect; speed=2500 rpm; preload=700 N

Figure 5 shows the vibration signal spectrum of normal bearing in the case that the rotating speed is 5000 rpm and the axial preload is 500 N. As indicated in this figure, the major features of the normal bearing are the vibration energy concentration at the shaft rotating frequency f_r and the cage rotating frequency f_c. Figure 6 shows the vibration signal spectrum of bearing with outer race defect in the case of rotating speed of 2500 rpm and axial preload of 700 N. It can be observed that except to the vibration energy concentration at f_c, and f_r, there is also a spectral peak near the frequency of the rolling ball passing through one point of the outer race, f_{bpo} due to the defect on the outer race. The vibration signal spectrum of bearing with inner race defect under the case of the

rotating speed of 5500 rpm and the axial preload of 500 N is shown in Figure 7. Similarly, it is noted that the obvious features of defect on inner race include the spectral peaks at the shaft rotating frequency f_r as well as its harmonics. The vibration energy concentration can be also found around the frequency of the rolling ball passing through one point of the inner race, f_{bpi}. Figure 8 shows the vibration signal spectrum of bearing with ball defect in the case of rotating speed of 1500 rpm and axial preload of 500 N. By observing the vibration energy around the major characteristic frequencies, it is found that the peaks locate around the shaft rotating frequency f_r, the ball spin frequency f_{bs}, the frequency of one point on the ball passing through raceways and cage f_{rp}, and the frequency of the rolling ball passing through one point of the outer race, f_{bpo}. The major features with regard to the rolling ball defect are not obvious relatively. The possible reasons are that the impact vibration induced by the rolling ball defect is relatively lower with compared to that of raceway defects, and the impact vibration between the ball defect and raceway may not happen due to the direction change of the defective rolling ball. In conclusion, the characteristic frequencies of the vibration measurements are close to those that are derived through the numerical solutions of contact angles under the different shaft rotating speeds and axial preloads. As shown in the experimental results, the numerically determined bearing characteristic frequencies have accuracy of more than 90%.

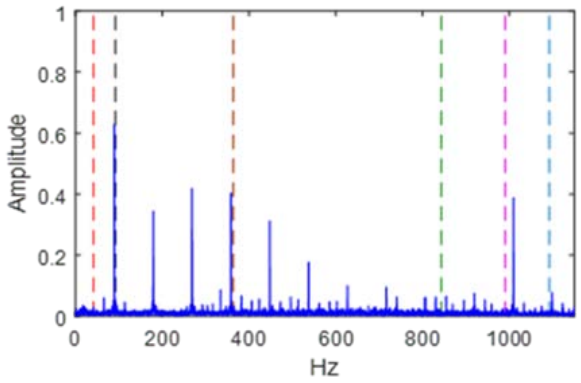

Figure 7 Spectrum of bearing with inner race defect; speed=5500 rpm; preload=500 N

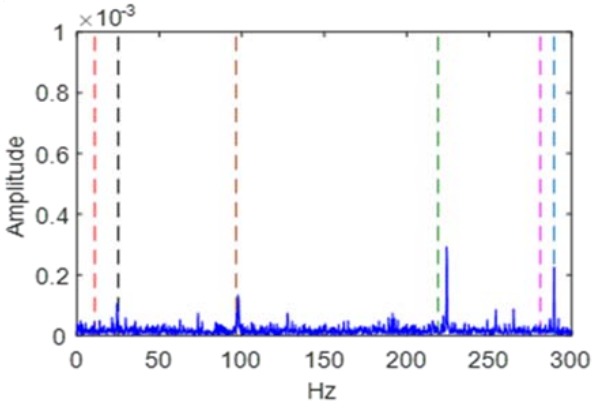

Figure 8 Spectrum of bearing with ball defect; speed=1500 rpm; preload=500 N

4. Conclusion

In this research, the theoretical dynamical model of angular-contact ball-bearing was formulated in terms of the bearing geometric relationship, force/moment equilibrium and point contact deformation derivation. The contact angles between the rolling ball and the inner/outer races were then resolved numerically based on the theoretical dynamical model through the GA optimization approach. The characteristic frequencies related to the bearing defects were determined according to the contact angle variations. The spectrum analysis of the experimental results was employed to observe the defective features of bearing. It is noted that the major features of bearing defects in the experiment are the vibration energy concentration at the corresponding characteristic frequencies which are close to the numerically determined values within a tolerace of 10%.

REFERENCES

1 Hertz, H. On the Contact of Elastic Solids, *J. Reine Angew. Math*, **92**, 156-171, (1881).
2 Stribeck, R. Ball Bearings for Various Loads, *Trans. ASME*, **29**, 420-463, (1907).
3 Jones, A. A General Theory for Elastically Constrained Ball and Radial Roller Bearings under Arbitrary Load and Speed Conditions, *Journal of Basic Engineering*, **82**, 309-320, (1960).
4 Harris, T. *Rolling Bearing Analysis*, 3rd ED., John Wiley and Sons, Inc., New York, (1991).
5 Brändlein, J. *Ball and Roller Bearings: Theory, Design and Application*, 3rd ED., John Wiley

and Sons, Inc., (1999).
6 Antoine, J. F., Abba, G. and Molinari, A. A new proposal for Explicit Angle Calculation in Angular Contact Ball Bearing, *Journal of Mechanical Design*, **128**, 468-478, (2006).
7 Houpert, L. A Uniform Analytical Approach for Ball and Roller Bearings Calculations, *Journal of Tribology*, **119**, 851-858, (1997)
8 Huang, N. E., Shen, Z., Long, S. R., Wu, M. C., Shih, H. H., Zheng, Q., Yen, N.-C., Tung, C. C. and Liu, H. H. The Empirical Mode Decomposition and the Hilbert Spectrum for Nonlinear and Non-stationary Time Series Analysis, *Proceedings of Royal Society London A*, **454**, 903–995, (1998).